Volume 1 | Number 1 | Jan 2013 | Pages 1–100

Dalton Transactions

An international journal of inorganic chemistry
www.rsc.org/dalton

ROYAL SOCIETY OF CHEMISTRY

ROYAL SOCIETY OF CHEMISTRY

www.rsc.org/dalton

Journal Name

Photocatalytic reactivity tuning by heterometal and addenda metal variation in Lindqvist polyoxometalates

Johannes Tucher,[a] Stefanie Schlicht,[b] Fabian Kollhoff[b] and and Carsten Streb*[a,b]

ABSTRACT: A systematic study into the effects of metal substitution on the visible-light photocatalytic activity of prototype metal oxide cluster anions is presented. Four isostructural Lindqvist clusters $[V_xM_{6-x}O_{19}]^{(2+x)-}$ (M = W, Mo, x = 1-2) with photooxidative activity in the visible range are reported. It is shown that the photooxidative performance correlates with the number of vanadium atoms in the cluster. Further, two divergent reaction mechanism are observed depending on the type of *addenda* metal (i.e. Mo or W) used. When comparing reactivity under aerated vs. de-aerated conditions, it was found that molybdate-based clusters show significantly increased reaction rates in the absence of oxygen; in contrast, marginally reduced reaction rates were observed for the tungstate-based species under de-aerated conditions. Wavelength-dependent quantum efficiency studies provide insight into the visible-light reactivity of all four species. Radical scavenging experiments suggest that the photocatalysis proceeds *via* formation of hydroxyl radicals. Cluster recycling studies demonstrate the robust nature of the homogeneous photocatalysts.

Introduction

The design of photoactive metal oxides is often limited to materials where light absorption is mainly based in the UV-region.[1] This is due to a large HOMO-LUMO gap of the O→M ligand-to-metal charge-transfer (LMCT) transitions which form the basis of metal oxide photochemistry.[2] Thus, sunlight driven photocatalyst development based on metal oxides is still a major challenge.[3-5] However, one possible route is the development of molecular metal oxides, so-called polyoxometalates (POMs). POMs are high-valent metal oxide clusters formed by self-assembly of small oxometalate precursors such as VO_4^{3-}, MoO_4^{2-} and WO_4^{2-}.[6-10] POMs combine key features of solid-state metal oxides with the structural and chemical tunability intrinsic to molecular materials.[11] For this reason, POMs have been extensively used as functional molecular materials in catalysis,[12, 13] photocatalysis,[14, 15], redox-active functional materials,[16] and energy conversion and storage.[17-20] The chemical and structural modification of POMs can be achieved by tuning the secondary reaction parameters (e.g. solution pH, reaction temperature, etc.) during cluster self-assembly.[6, 7] This approach can also be transferred to the development POM photocatalysts[14, 15] as the electronic properties of the clusters (and therefore their visible-light photoactivity) is controlled by the underlying cluster structure.[21-26] Based on this concept, functionalization routes were developed where selective metal substitution is used to photosensitize clusters in the visible.[23, 24, 26, 27] Thus far, the concept of metal-substituted POM photocatalysts has mainly been focused on Keggin derivatives $[XM_{12}O_{40}]^{n-}$ (M = V, Mo, W)[28, 29] whereas the development of other heterometallic, photoactive POM clusters is still in its infancy.[30, 31]

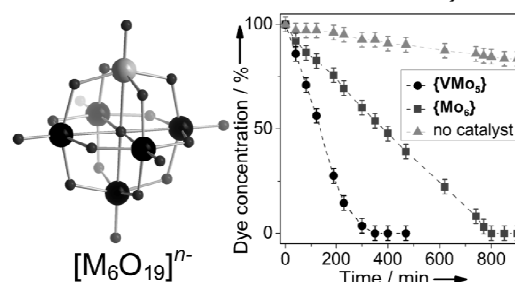Figure 1. Left: Illustration of the Lindqvist architecture $[M_6O_{19}]^{n-}$.[24] Right: Photooxidative performance of {**Mo₆**} and {**VMo₅**} in the photooxidation of the model pollutant dye patent blue V under broadband UV irradiation.

Based on this background, we started to investigate small prototype clusters[24] where selective metal exchange can be used to tune the electronic cluster properties whilst retaining the physical cluster architecture. We identified Lindqvist clusters[10] $[M_6O_{19}]^{n-}$ (M = Mo, W (n= 2); Ta, Nb (n= 8))[32, 33] as prime model systems since their chemical modification by metal substitution is well established. Consequently, a family of heterometallic Lindqvist clusters $[M'(L)M_5O_{18}]^{n-}$ (M = Mo, W; M' = transition metal, *e.g.* Co, V, Zr, Hf, L= ligand, e.g. RO⁻, O^{2-}, *etc.*) is known to-date.[34-38]

Recently, we used this synthetic concept to compare the photocatalytic performance of the non-functionalized molybdate Lindqvist $[Mo_6O_{19}]^{2-}$ ({**Mo₆**}) with the mono-vanadium-substituted cluster $[VMo_5O_{19}]^{3-}$ (= {**VMo₅**}), see Fig. 1.[24] Photocatalytic tests showed that under UV and visible light irradiation, higher photoactivity was found for {**VMo₅**} than for {**Mo₆**}. At high wavelengths (λ > 450 nm), {**Mo₆**} was photochemically inactive whereas {**VMo₅**} still showed photooxidative activity, confirming that metal substitution is a powerful tool for tuning the visible light photoactivity of small POM clusters.

In the current report, this strategy was significantly broadened by expanding the cluster family to vanadium-functionalized molybdate and tungstate clusters and introducing mono- and di-vanadium functionalized clusters.[38] A summary of the photocatalysts under investigation is given in Table 1.

Table 1. Summary of the photocatalysts used

No	Formula	Abbreviation
1	$(nBu_4N)_3[VMo_5O_{19}]$	{**VMo₅**}
2	$(nBu_4N)_3[VW_5O_{19}]$	{**VW₅**}
3	$(nBu_4N)_3Na[V_2Mo_4O_{19}]$	{**V₂Mo₄**}
4	$(nBu_4N)_3Na[V_2W_4O_{19}]$	{**V₂W₄**}

Here, the performance of **1-4** was investigated using the photooxidation of indigo (Ind) as the benchmark reaction. Several aspects of the photooxidation mechanism such as presence of oxygen, presence of hydroxyl radical scavengers, wavelength-dependent quantum efficiencies and cluster recycling were studied to identify the most promising reaction systems.

Results and Discussion

Synthesis and characterization

Compounds **1-4** were obtained by modified literature syntheses (see SI for details).[38] The compounds were isolated as organo-soluble salts using tetra-*n*-butylammonium counter ions. The compounds were characterized using high-resolution electrospray ionization mass spectrometry, elemental analysis and flame atomic absorption spectroscopy, for details see and SI.

UV-Vis spectroscopy

UV-Vis spectroscopy of **1-4** showed that all clusters feature O-M LMCT transitions in the UV range which extend into the visible

region. Notably, vanadium incorporation results in increased visible light absorption and tailing of the near UV/Vis transitions up to λ *ca.* 520 nm was observed. In a previous report we showed that the visible light absorption is mainly arising from O-V LMCT transitions.[24] Notably, {**VMo₅**} shows the lowest light absorption in the visible range between λ = 400 – 500 nm amongst the compounds investigated, see Fig. 2. The clusters also show distinct band features in the UV range between 300-400 nm, suggesting that the electronic cluster structure is significantly altered by vanadium incorporation.

Photocatalytic studies

Comparative photooxidation studies were performed to evaluate the photooxidative activity of **1-4**. To this end, **1-4** were dissolved in N,N-dimethyl formamide (DMF) and aliquots of the model substrate indigo (Ind) were added at molar ratios [Ind] : [cluster] = 5 : 1. The homogeneous solutions were irradiated using a LED light source (λ= 430 nm) in custom-built irradiation setups. Photooxidation kinetics were followed spectrometrically, see Fig. 3.
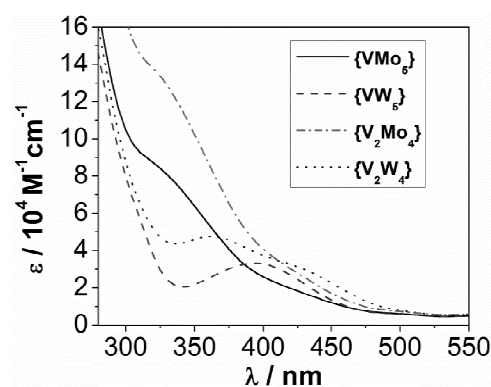

Figure 2. UV-Vis spectra of compounds **1-4** in DMF, showing the effect of vanadium substitution on the visible light absorption.

Aerated conditions

Initial experiments were focused on the performance of **1-4** under aerated conditions and obvious differences in the photooxidation kinetics were observed depending on the cluster employed. From Figure 3, two distinct trends are obvious: (**1**) Significantly faster reaction kinetics are observed for the tungstate species {**VW₅**} and {**V₂W₄**} compared with the molybdates {**VMo₅**} and {**V₂Mo₄**}, see Table 2. In addition, the tungstate-based species show pseudo-first order kinetics, whereas the molybdate species feature pseudo-zeroth order kinetics. (**2**) Slightly faster reaction kinetics are observed for the di-vanadium functionalized clusters {**V₂Mo₄**} and {**V₂W₄**} compared to the mono-vanadium species {**VMo₅**} and {**VW₅**}. Quantitative insight was obtained by determining the initial observed rate constants k_{obs} using a zeroth-order model; this data is summarized in Table 2.

De-aerated conditions

Next, the indigo photooxidation was investigated under de-aerated conditions; this was based on previous findings where significant oxygen-related effects on the photoreactivity of

POMs were reported.[24] To this end, the standard photooxidation conditions (see above) were used, but the samples were de-aerated by flushing with Argon for 10 min prior to the experiment. During the photooxidation, the samples were kept under Argon. Data analysis shows that a significant increase in reaction rate is observed for the molybdate-based clusters {VMo$_5$} (+ 406 %) and {V$_2$Mo$_4$} (+ 326 %); see Table 2. In contrast, for the tungstate-based clusters, the observed reaction rate is only marginally affected and a minor decrease is found: {VW$_5$} (- 16 %) and {V$_2$W$_4$} (- 10 %). In consequence, under de-aerated conditions, the molybdate-based species are the

more active photocatalysts. Notably, this observation suggests that different photooxidation mechanisms are present for the molybdate- and tungstate-based species, respectively. The photoactivity of the molybdate species is significantly reduced in the presence of oxygen, suggesting an oxygen-dependent quenching mechanism (possibly proceeding *via* $^3O_2$ triplet quenching[39]) which limits their activity under aerated conditions. In contrast, the tungstate-based species are only marginally affected by the presence of oxygen, resulting in their superior performance under aerated conditions.[24]

Table 2. Summary of the photooxidation parameters observed for the indigo photooxidation by **1-4**.[a]

	Compound	Aerated k_{obs} / µM h^{-1}[d]	De-aerated[b] k_{obs} / µM h^{-1}[d]	Hydroxyl scavenger present (EtOH)[c]	
				k_{obs} / µM h^{-1} (aerated)[d]	k_{obs} / µM h^{-1} (de-aerated)[d]
	Blank[e]	0.27 ± 0.06	0.24 ± 0.08	0.11 ± 0.01	0.12 ± 0.03
1	{VMo$_5$}	2.56 ± 0.04	10.40 ± 0.58	1.31 ± 0.11	2.02 ± 0.17
2	{VW$_5$}	7.61 ± 0.38	6.41 ± 0.31	2.14 ± 0.18	2.07 ± 0.11
3	{V$_2$Mo$_4$}	3.29 ± 0.10	10.70 ± 0.35	1.85 ± 0.21	2.72 ±0.22
4	{V$_2$W$_4$}	8.48 ± 0.48	7.64 ± 0.25	2.35 ± 0.17	2.39 ± 0.20

[a] Conditions: solvent: DMF, [Ind] : [cluster] = 5:1, LED light source, λ = 430 nm. [b] samples were de-aerated by flushing with Argon for 10 min prior to the experiment. [c] [EtOH] : [Ind] : [cluster] = 50 : 5 : 1. [d] k_{obs} = initial observed rate constant (zeroth order model); [e] blank = identical reaction conditions, no photocatalyst present
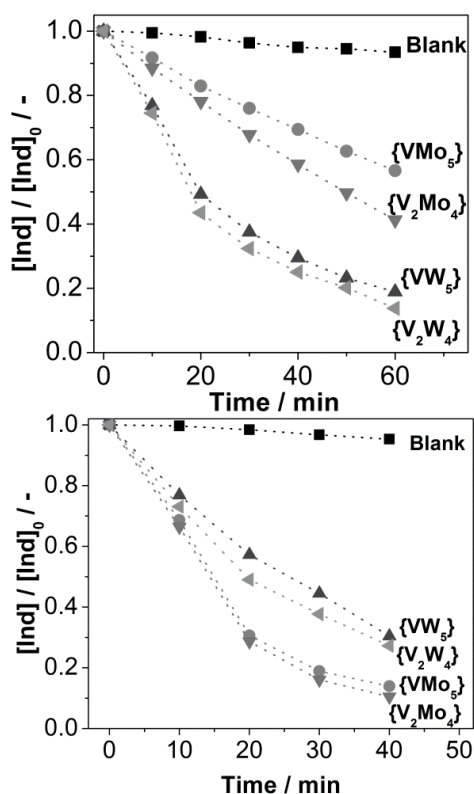

Figure 3. **Top:** Photooxidation of indigo (Ind) by **1-4** under aerated conditions. Significantly faster kinetics are observed for {VW$_5$} and {V$_2$W$_4$} compared with {VMo$_5$} and {V$_2$Mo$_4$}. **Bottom:** Ind photooxidation by **1-4** under de-aerated

conditions. Significantly increased reaction rates are observed for {VMo$_5$} and {V$_2$Mo$_4$}. For {VW$_5$} and {V$_2$W$_4$}, a minor decrease in reaction rate is observed. Conditions: solvent: DMF, [Ind] : [cluster] = 5:1, LED light source, λ = 430 nm. De-aerated samples were flushed with Ar for 10 min prior to the experiment.

Effect of hydroxyl radical scavengers

The effects of hydroxyl radical scavengers on the photooxidation by **1-4** was investigated to establish whether hydroxyl radicals are involved in the photooxidation mechanism. This is based on previous work which showed that POM photooxidation typically proceeds *via* the intermediate formation of hydroxyl radicals by reaction of cluster-bound water molecules with the photoexcited cluster.[27]

To this end, the standard photooxidation reaction (see above) was performed in the presence of ethanol as a standard hydroxyl radical scavenger ([EtOH] : [Ind] : [cluster] = 50 : 5 : 1). The experiments were performed under aerated and de-aerated conditions and show almost identical behaviour: for all compounds, a significant decrease in photooxidative activity is observed (Table 2), suggesting that hydroxyl radical formation is indeed the basis of the photooxidation mechanism for all compounds under investigation.

Quantum efficiency

The wavelength-dependent quantum efficiencies of **1-4** for the aerated photooxidation of indigo were determined under monochromatic light irradiation to assess the cluster performance.[40] Measurements were performed using a custom-built system in the range of λ = 395 - 505 nm. Quantum

efficiencies were found to be below 1 %, highlighting that the photochemically most active bands of the clusters are still in the UV region, see Table 3. The data show that higher quantum efficiencies are found for the di-vanadium substituted units $\{V_2Mo_4\}$ and $\{V_2W_4\}$ and quantum efficiency decreases with increasing wavelength (Fig. 4).
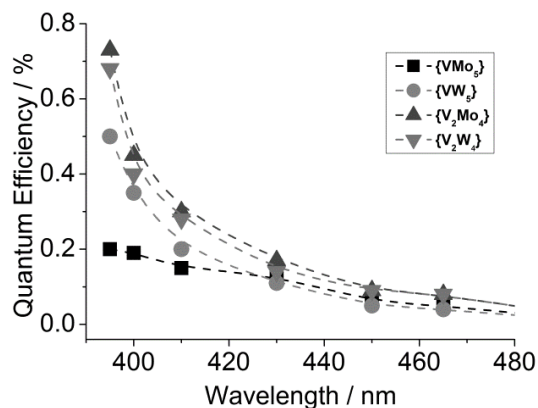

Figure 4. Quantum efficiencies in the visible range for the indigo photooxidation by **1-4**. At the UV-Vis border, higher quantum efficiencies for the di-vanadium-substituted species are observed. The tailing of the quantum efficiencies at higher wavelengths correlates with the decreasing cluster absorptivity. Conditions: solvent: DMF, [Ind]:[cluster] = 1:1; [Ind] = [cluster] = 1.0 μM ;

Table 3. Quantum efficiencies φ for **1-4** observed in the photooxidation of indigo[a]

λ / nm	$\phi(\{VMo_5\})$ / %	$\phi(\{VW_5\})$ / %	$\phi(\{V_2Mo_4\})$ / %	$\phi(\{V_2W_4\})$ / %
395	0.2	0.5	0.73	0.68
400	0.19	0.35	0.45	0.4
410	0.15	0.2	0.3	0.28
430	0.13	0.11	0.17	0.14
450	0.11	0.05	0.09	0.09
465	0.1	0.04	0.08	0.08
505	0	0	0	0

[a] Conditions: solvent: DMF, [Ind]:[cluster] = 1:1; [Ind] = [cluster] = 1.0 μM

Cluster recycling

Recycling experiments were performed by conducting the standard Ind photooxidation (see above). After dye photooxidation was complete, a second aliquot of indigo was added and the photooxidation was repeated. Overall, three runs were performed under identical conditions and only marginal decrease in dye photooxidation kinetics was observed (see SI), suggesting that the clusters can be employed as photooxidation catalysts multiple times. Changes in the relative cluster performance over several runs are observed (e.g. decreasing

rate constant for $\{VW_5\}$ under aerated conditions) which are currently under investigation.

Conclusions

In summary, we illuminate the effects of *addenda* metal and *heterometal* on the photocatalytic performance of mixed-metal polyoxometalates: using four isostructural Lindqvist clusters $[V_xM_{6-x}O_{19}]^{(2+x)-}$ (M = W, Mo, x = 1-2) as prototypes, we report that all compounds show photoactivity up to *ca.* 450 nm and are active photooxidation catalysts. A striking difference in photoreactivity is observed when comparing tungstate- and molybdate-based clusters: under de-aerated conditions, a significant increase in photoreactivity (up to *ca.* 400 %) is observed for the molybdate-based species. In contrast, de-aerated conditions result in a minor decrease in photoreactivity (< *ca.* 20 %) for the tungstate clusters. Under aerated conditions, the tungstate-based systems feature higher reactivity than the molybdate systems. The findings suggest that oxygen quenches photoreactivity for the molybdates but not for the tungstates and two different reaction mechanisms must therefore be present. Further, mechanistic studies show that all four compounds feature drastically reduced reactivity in the presence of, hydroxyl radical scavengers, providing evidence that OH radicals are formed as reactive intermediates during irradiation.

Future work will use photophysical and computational analyses so as to determine the underlying mechanism of the divergent reactivity of molybdate and tungstate Lindqvists.. The clusters will be screened for use in technologically relevant photooxidation reactions such as alcohol and olefin oxidations.

Acknowledgements

Notes and references

[a] Ulm University, Institute of Inorganic Chemistry I, Albert-Einstein-Allee 11, 89081 Ulm, Germany. carsten.streb@uni-ulm.de

[b] Department Chemistry and Pharmacy, Friedrich-Alexander-University Erlangen-Nuremberg, Egerlandstr. 1, 91058 Erlangen, Germany.

† For synthetic details of compounds **1-4**, see ESI.

Elemental analysis for **1**: $C_{48}H_{108}N_3VMo_5O_{19}$ (Mw: 1562.02 g/mol) in wt.-% (calcd.): C 37.09 (36.91), H 7.15 (6.97), N 2.84 (2.69), V 2.62 (3.24), Mo 31.91 (31.16). Cluster anion observed in ESI-MS: 1077.66 (calcd: 1077.68), assigned as $\{(nBu_4N)H[VMo_5O_{19}]\}^-$.

Elemental analysis for **2**: $C_{48}H_{108}N_3VW_5O_{19}$ (Mw: 2001.52 g/mol) in wt.-% (calcd.): C 29.07 (28.80), H 5.52 (5.44), N 2.12 (2.10), V 2.04 (2.55), W 45.31 (45.93). Cluster anion observed in ESI-MS: 1759.15 (calcd: 1759.16), assigned as $\{(nBu_4N)_2VW_5O_{19}\}^-$.

Elemental analysis for **3**: C48H108N3NaV2Mo4O19 (Mw: 1540.01 g/mol) in wt.-% (calcd.): C 37.04 (37.44), H 7.03 (7.07), N 2.70 (2.73), Na 1.38 (1.49), V 6.12 (6.62), Mo 24.79 (24.92). Cluster anion observed

in ESI-MS: 1319.91 (calcd: 1319.89), assigned as $\{(nBu_4N)_2(MeCN)_5Na(H_2O)_6[V_2Mo_4O_{19}]\}^-$.

Elemental analysis for **4**: $C_{48}H_{108}N_3NaV_2W_4O_{19}$ (Mw: 1891.61 g/mol) in wt.-% (calcd.): C 30.04 (30.48), H 5.73 (5.75), N 2.18 (2.22), Na 1.12 (1.22) V 7.08 (7.09), W 50.79 (51.14). Cluster anion observed in ESI-MS: 606.84 (calcd: 606.84), assigned as $\{(NH_4)_2(H_2O)_2V_2W_4O_{19}\}^{2-}$.

Photocatalytic measurements: the standard indigo photooxidation was carried out as follows: a N,N-dimethyl formamide (DMF) solution of the respective cluster (1.0 μM) and and indigo (5.0 μM) was prepared. The homogeneous solution was irradiated with a custom built LED irradiation setup (standard light source: λ = 430 nm, $P_{nominal}$ = 3 W, other wavelengths are stated in the text). Indigo photooxidation was detected spectrometrically by following the decrease of the characteristic absorption signal at λ_{max} = 609 nm. De-aerated experiments were performed by flushing the sample with Ar for 10 min prior to the experiment. Hydroxyl radical scavenging experiments were performed by adding ethanol (50 μM) to the solution.

Electronic Supplementary Information (ESI) available: experimental, analytical and catalytic details are given. See DOI: 10.1039/b000000x/

1. R. van de Krol, Y. Liang and J. Schoonman, *J. Mater. Chem.*, 2008, **18**, 2311-2320.
2. H.-J. Zhai, J. Döbler, J. Sauer and L.-S. Wang, *J. Am. Chem. Soc.*, 2007, **129**, 13270-13276.
3. K. Hashimoto, H. Irie and A. Fujishima, *Jpn. J. Appl. Phys.*, 2005, **44**, 8269.
4. D. Zhang, G. Li, H. Li and Y. Lu, *Chem. Asian J.*, 2013, **8**, 26-40.
5. A. Kudo, *Pure Appl. Chem.*, 2007, **79**, 1917-1927.
6. D. L. Long, R. Tsunashima and L. Cronin, *Angew. Chem. Int. Ed.*, 2010, **49**, 1736-1758.
7. D. L. Long, E. Burkholder and L. Cronin, *Chem. Soc. Rev.*, 2007, **36**, 105-121.
8. Special POM issue: C. Hill (guest ed.), *Chem. Rev.*, 1998, **98**, 1.
9. M. T. Pope and A. Müller, *Angew. Chem. Int. Ed. Engl.*, 1991, **30**, 34-48.
10. M. T. Pope, *Heteropoly and isopoly oxometalates*, Springer-Verlag, Heidelberg, 1983.
11. Special POM issue: L. Cronin and A. Müller (guest eds.), *Chem. Soc. Rev.*, 2012, **41**, 7325-7648.
12. C. L. Hill and C. M. Prosser-Mccartha, *Coord. Chem. Rev.*, 1995, **143**, 407-455.
13. C. L. Hill, *J. Molec. Catal. A*, 2007, **262**, 2-6.
14. C. L. Hill and C. M. Prosser-McCartha, in *Photosensitization and Photocatalysis using inorganic and organometallic compounds*, eds. M. Graetzel and K. Kalyanasundaram, Kluwer Academic Publishers, Dordrecht, 1993, pp. 307-326.
15. E. Papaconstantinou and A. Hiskia, in *Polyoxometalate Molecular Science*, eds. J. J. Borras-Almenar, E. Coronado, A. Mueller and M. T. Pope, Kluwer Academic Publishers, Dordrecht, 2003, pp. 381-416.
16. S. G. Mitchell, C. Streb, H. N. Miras, T. Boyd, D.-L. Long and L. Cronin, *Nat. Chem.*, 2010, **2**, 308-312.
17. B. Botar, Y. V. Geletii, P. Kögerler, D. A. Hillesheim, D. G. Musaev and C. L. Hill, *Angew. Chem. Int. Ed.*, 2008, **47**, 3896-3899.
18. Y. V. Geletii, Z. Q. Huang, Y. Hou, D. G. Musaev, T. Q. Lian and C. L. Hill, *J. Am. Chem. Soc.*, 2009, **131**, 7522-7524.
19. A. Sartorel, M. Carraro, G. Scorrano, R. De Zorzi, S. Geremia, N. D. McDaniel, S. Bernhard and M. Bonchio, *J. Am. Chem. Soc.*, 2008, **130**, 5006-5009.
20. Q. S. Yin, J. M. Tan, C. Besson, Y. V. Geletii, D. G. Musaev, A. E. Kuznetsov, Z. Luo, K. I. Hardcastle and C. L. Hill, *Science*, 2010, **328**, 342-345.
21. X. Lopez, J. J. Carbo, C. Bo and J. M. Poblet, *Chem. Soc. Rev.*, 2012, **41**, 7537-7571.
22. J. Forster, B. Rösner, M. M. Khusniyarov and C. Streb, *Chem. Commun.*, 2011, **47**, 3114-3116.
23. (a) J. Tucher, L. C. Nye, I. Ivanovic-Burmazovic, A. Notarnicola and C. Streb, *Chem. Eur. J.*, 2012, **18**, 10949-10953; (b) J. Tucher and C. Streb, *Beilstein J. Nanotechnol.* 2014, **5**, 711-716.
24. J. Tucher, Y. L. Wu, L. C. Nye, I. Ivanovic-Burmazovic, M. M. Khusniyarov and C. Streb, *Dalton Trans.*, 2012, **41**, 9938-9943.
25. C. Streb, K. Kastner and J. Tucher, in *Chemical Photocatalysis*, ed. B. König, De Gruyter, Berlin, 2013, pp. 247-258.
26. A. Seliverstov and C. Streb, *Chem. Commun.*, 2014, **50**, 1827-1829.
27. C. Streb, *Dalton Trans*, 2012, **41**, 1651-1659.
28. C. L. Hill, in *Comprehensive Coordination Chemistry II*, eds. J. A. McCleverty and T. J. Meyer, Elsevier, Oxford, 2004, vol. 4, pp. 679-759.
29. E. N. Glass, J. Fielden, A. L. Kaledin, D. G. Musaev, T. Lian and C. L. Hill, *Chem. Eur. J.*, 2014, **20** 4297–4307.
30. J. Ettedgui, Y. Diskin-Posner, L. Weiner and R. Neumann, *J. Am. Chem. Soc.*, 2011, **133**, 188-190.
31. A. M. Khenkin, I. Efremenko, L. Weiner, J. M. L. Martin and R. Neumann, *Chem. Eur. J.*, 2010, **16**, 1356-1364.
32. M. Nyman, *Dalton Trans.*, 2011, **40**, 8049-8058.
33. T. M. Anderson, M. A. Rodriguez, F. Bonhomme, J. N. Bixler, T. M. Alama and M. Nyman, *Dalton Trans.*, 2007, 4517-4522.
34. R. J. Errington, L. Coyle, P. S. Middleton, C. J. Murphy, W. Clegg and R. W. Harrington, *J. Clust. Sci.*, 2010, **21**, 503-514.
35. R. J. Errington, G. Harle, W. Clegg and R. W. Harrington, *Eur. J. Inorg. Chem.*, 2009, 5240-5246.
36. R. J. Errington, S. S. Petkar, P. S. Middleton and W. McFarlane, *J. Am. Chem. Soc.*, 2007, **129**, 12181-12196.
37. R. J. Errington, S. S. Petkar, B. R. Horrocks, A. Houlton, L. H. Lie and S. N. Patole, *Angew. Chem. Int. Ed.*, 2005, **44**, 1254-1257.
38. M. Filowitz, R. K. C. Ho, W. G. Klemperer and W. Shum, *Inorg. Chem.*, 1979, **18**, 93-103.
39. L. Patterson, G. Porter and M. Topp, *Chem. Phys. Lett.*, 1970, **7**, 612-614.
40. U. Megerle, R. Lechner, B. Konig and E. Riedle, *Photochem. Photobiol. Sci.*, 2010, **9**, 1400-1406.

Dalton Transactions Accepted Manuscript
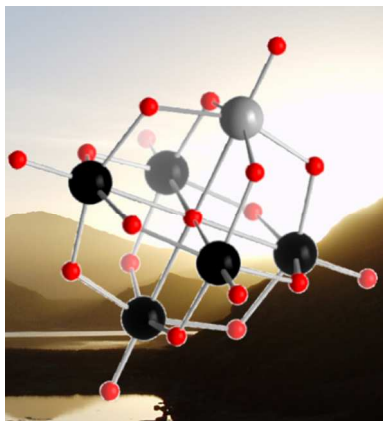
The photooxidative performance of a family of mixed-metal oxide Lindqvist clusters $[V_xM_{6-x}O_{19}]^{(2+x)-}$ (M = W, Mo, x = 1-2) is presented. Mono- and di-vanadium incorporation increases the visible-light photoactivity. Divergent reaction mechanisms are observed depending on the type of *addenda* metal (i.e. Mo/W) used.